

# Molecular Mechanism of Swing Effect in Zeolitic Imidazolate Framework ZIF-8: Continuous Deformation upon Adsorption

François-Xavier Coudert<sup>\*[a]</sup>

Zeolitic imidazolate framework ZIF-8 displays flexibility of its structure by rotation of its imidazolate linker. This “swing effect” has been widely described in the literature, both experimentally and theoretically, as a bistable system where the linker oscillates between two structures: “open window” and “closed window”. By using quantum chemistry calculations and first-principles molecular dynamics simulations, it is shown that

the deformation upon adsorption is in fact continuous upon pore loading, with thermodynamics of packing effects being the reason behind stepped adsorption isotherms experimentally observed. Finally, we study a variant of ZIF-8 with a different linker, highlighting the influence of the linker and the balance of microscopic interactions on the framework's flexibility.

## 1. Introduction

Zeolitic imidazolate frameworks (ZIF) are a subclass of metal-organic frameworks (MOF)<sup>[1–4]</sup> formed from imidazolate linkers and metal cations, linked together into three-dimensional zeolitic frameworks.<sup>[5–8]</sup> Like MOFs, ZIFs feature tunable nanoporosity (e.g., by changing the size of their linker), structural flexibility (dictated by relatively weak coordination bonds and intermolecular forces), and versatility of their inner surface (through functionalization of the organic ligand). They also feature strengths typical of the zeolites family, in terms of thermal, mechanical and chemical stability. Finally, due to the large diversity of four-connected nets, over 100 different ZIF structures have been reported so far, with many more potential structures existing within a small range of enthalpy of formation.<sup>[9–11]</sup> ZIFs present a great potential for applications such as gas capture (CO<sub>2</sub> in particular),<sup>[12]</sup> sensing,<sup>[13]</sup> encapsulation and controlled delivery,<sup>[14]</sup> and fluid separation.<sup>[15–18]</sup>

ZIF-8, in particular, is commercially available, has been widely studied, and has excellent performance at lab scale for the separation of many strategic mixtures, including C<sub>2</sub>/C<sub>3</sub> hydrocarbons, CO<sub>2</sub>/CH<sub>4</sub>, CO<sub>2</sub>/N<sub>2</sub>, biobutanol fermentation mixture, phenolic isomers, etc. It is a low density porous framework with the sodalite (**sod**) topology and chemical formula Zn(*mim*)<sub>2</sub>, where *mim* = 2-methylimidazolate (see Figure 1). It features large spherical cages, called sodalite cages, separated by 6-ring windows of small aperture ( $\approx 3.4$  Å diameter as determined from the crystallographic structure), and 4-rings that connect different cages. It has high thermal, mechanical and

chemical stability,<sup>[5,19]</sup> and can be readily assembled into membranes<sup>[20]</sup> or form thin films.<sup>[21]</sup> It undergoes amorphization under mechanical pressure<sup>[22]</sup> or ball milling.<sup>[23]</sup>

Moreover, studies have highlighted that ZIF-8 exhibits some flexibility of its framework in the form of a torsional motion of its imidazolate linkers, a phenomenon called the “swing effect”. Both experimental and theoretical works on ZIF-8 have noted a discrepancy between experimental results of gas adsorption and diffusivity, and the values that could be predicted from molecular simulations in rigid structures or simple considerations comparing the ZIF-8 window size and the adsorbates' kinetic diameter.<sup>[24]</sup> This ability of molecules larger than the geometric window size to diffuse through the ZIF-8 framework was attributed to flexibility of the structure.<sup>[25]</sup> The best-documented evidence of this effect was the computational characterization of self and transport diffusion coefficients of methane, ethane, ethylene, propane, propylene, *n*-butane, and 1-butene, by the Sholl group.<sup>[26]</sup> By comparing simulation results to experimental transport properties, the authors showed that framework flexibility plays a critical role in accurately describing molecular diffusion.

Moreover, there is ample direct evidence of a structural transition occurring in ZIF-8 upon loading, first reported by Moggach et al. in an high-pressure experiment using a methanol/ethanol mixture as hydrostatic medium.<sup>[27]</sup> They demonstrated that at a pressure of 1.47 GPa, the intrusion of methanol molecules into the ZIF-8 nanopores triggers a reversible single-crystal to single-crystal structural transition. The “high pressure” (or HP) phase has the same space group (*I* $\bar{4}$ 3*m*) as ZIF-8, a slightly larger unit cell volume (4974.8 Å<sup>3</sup> vs. 4900.5 Å<sup>3</sup>), and exhibits a reorientation of the imidazolate linkers, which open the 6-ring windows. In later work, Fairen-Jimenez et al.<sup>[28]</sup> demonstrated by in situ powder XRD measurements that the HP phase of ZIF-8 can also be observed upon adsorption of N<sub>2</sub> at 77 K. These authors also demonstrated that the stepped N<sub>2</sub> adsorp-

[a] Dr. F.-X. Coudert  
Chimie ParisTech, PSL Research University  
CNRS, Institut de Recherche de Chimie Paris  
75005 Paris (France)  
E-mail: fx.coudert@chimie-paristech.fr

Supporting Information and the ORCID identification number(s) for the author(s) of this article can be found under:  
<https://doi.org/10.1002/cphc.201700463>.

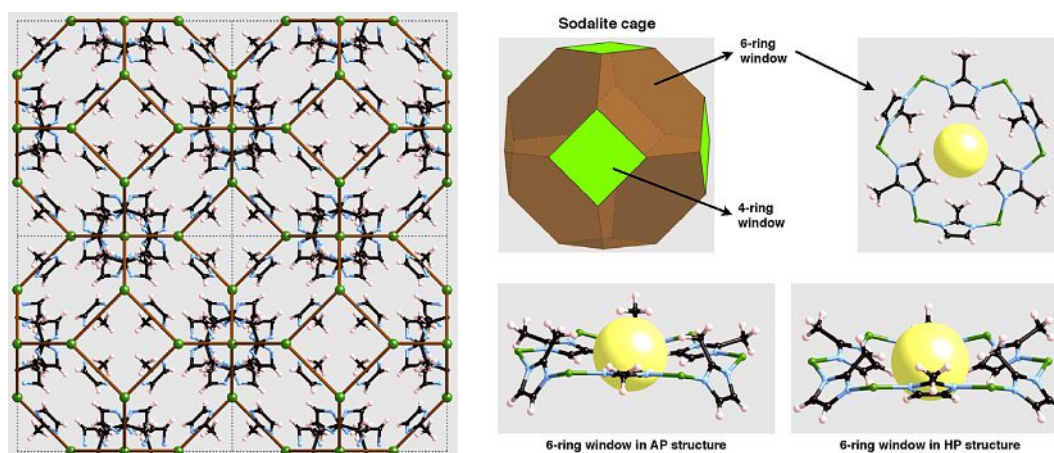


**Figure 1.** Left: representation of a  $2 \times 2$  supercell of the ZIF-8 structure, highlighting the SOD topology of the framework with brown lines drawn between neighboring  $\text{Zn}^{2+}$  ions (in green). Top right: views of the six-ring windows of ZIF-8's sodalite cages, and the window as viewed from above in the AP structure. Bottom right: lateral views in the AP and HP structures, showing the deformation of the window and reorientation of the 2-methylimidazolate linkers.

tion isotherm (at 77 K) could not be explained by Grand Canonical Monte Carlo (GCMC) simulations in a rigid “ambient pressure” (AP) ZIF-8 structure. They showed, on the contrary, that its lower pressure part matches the GCMC simulations performed in the AP structure, while the saturation uptake corresponded with GCMC simulations in the (rigid) HP structure.

Some of the same authors later studied adsorption of  $\text{CO}_2$ ,  $\text{CH}_4$ , and longer alkanes in ZIF-8, at temperatures between 120 and 300 K.<sup>[29]</sup> While no clear step can be seen on these experimental isotherms, they used GCMC simulations and Density Functional Theory (DFT) calculations to prove that adsorption could not be fully described by the AP structure only, but that two different structural configurations (AP and HP) of ZIF-8 are needed to properly describe the adsorption performance of this material. In particular, they demonstrated that the HP structure presents an additional adsorption site within its 4-ring window.

Finally, another study provided high-resolution adsorption and desorption isotherms of  $\text{CO}$ ,  $\text{N}_2$ ,  $\text{O}_2$  and Ar at 77 and 90 K, which all exhibit multiple steps as well as a hysteresis loop in the higher-pressure step.<sup>[30]</sup> As in the earlier work on  $\text{N}_2$ , Ania et al. compared these experimental isotherms to GCMC calculations performed on the rigid AP and HP structures, and attributed the stepped adsorption behavior to the packing arrangement of the guest molecules, as governed by polarizability, molecular size and shape of the gases.

However, while the thermodynamics and energetics of the ZIF-8 swing effect have been studied from the energetics and thermodynamics of adsorption in the two crystallographic structures AP and HP, little has been said of the nature of this structural transformation, what happens in between, and what is the dynamics of imidazolate linker swing motion in the material in the presence of adsorbate. To our knowledge, no experimental data or molecular simulation on the single-crystal to single-crystal AP  $\rightarrow$  HP transformation has determined whether it is a continuous deformation of the ZIF-8 structure, a phase transition between metastable phases of the material

(like the MIL-53 breathing transition, for example), or a “gate opening” phenomenon.

Finally, there is little information in the literature about the swing effect of the imidazolate linkers in other ZIFs of the *sod* topology, and the possible influence of linker functionalization on the framework dynamics. In the case of ZIF-7, a  $\text{Zn}(\text{benzenimidazolate})_2$  framework with great separation potential, the existence of a structural transformation was established by Aguado et al.,<sup>[31]</sup> and van den Bergh et al.<sup>[32]</sup> were able to give some microscopic insight into the energetics of adsorption of hydrocarbons in ZIF-7. Zhao et al.<sup>[33]</sup> determined the crystallographic structure of ZIF-7-II, obtained from ZIF-7 upon solvent evacuation, and showed that a dense phase with the same topology, ZIF-7-III, can also be triggered in the presence of water. Later, Du et al. showed the existence of a high-temperature transition, and elucidated the interplay between temperature effects and  $\text{CO}_2$  guest adsorption by establishing the phase diagram of ZIF-7 in  $(T, P_{\text{CO}_2})$  parameter space.<sup>[34]</sup>

Finally, the Hupp group<sup>[35]</sup> was able to obtain a ZIF of *sod* topology with unsubstituted imidazolate (*im*) as linked through solvent-assisted linker exchange: the resulting material, SALEM-2, incorporates as much as 85% of *im* versus *mim*. This change in the linker, while it has no bearing on the framework, appears to have an impact on the  $\text{N}_2$  adsorption properties. However, no detailed study of the imidazolate swing effect at the microscopic level has been performed.

In this paper, I look at the nature of the ZIF reorientation transition, and in particular whether it is a transition between two metastable phases of ZIF-8, a continuous adsorption-induced deformation, or a type of adsorbate-induced gate opening.<sup>[36]</sup> In order to bring microscopic insight into the transition, it is studied at the atomistic scale in terms of both energetics as well as thermal motion, with and without adsorbates. Because this effect is expected to be particularly difficult to capture with classical force fields and the strong assumptions they make on interatomic interactions, the issue is addressed through quantum chemistry simulations, using both zero

Kelvin energy minimizations and finite temperature molecular dynamics.

## 2. Results and Discussion

### 2.1. Quantum Chemistry Calculations

First, I performed quantum chemistry calculations starting from the experimental AP and HP structures, optimizing each structure's geometry—both atomic positions and unit cell parameters—in the absence of guests. The ZIF-8 AP structure is fairly well reproduced (see Table 1), but the HP structure spontaneously relaxes into AP, with extremely good precision. Thus, HP is not a metastable structure for the bare ZIF-8, that is, not a local minimum in the energy profile of the material. This is in contrast, for example, with adsorption-induced transitions such as the “breathing” transition in the MIL-53 family.<sup>[37]</sup>

**Table 1.** Properties (unit cell volume and cell parameters) of the ZIF-8 AP and HP phases, before and after DFT energy minimization in the absence of guest molecules.

Structure	Experimental volume used as starting point	Volume of DFT-relaxed structure	Unit cell parameter <i>a</i>
ZIF-8 AP	4907.12 Å <sup>3</sup>	4790.62 Å <sup>3</sup>	16.85766 Å
ZIF-8 HP	5006.60 Å <sup>3</sup>	4790.54 Å <sup>3</sup>	16.85756 Å

Then, I tried to see if the HP structure could be observed by applying pure (isotropic) mechanical stress to ZIF-8. To mimic the effect of adsorption-induced stress near saturation uptake (i.e. at large loading), where the HP structure is experimentally observed, I studied the effect of negative (outward) pressure on ZIF-8. Starting from the relaxed AP structure, an isotropic stress is applied and the deformation is measured (see Figure S1). A linear elastic domain is found up to  $P = -1.5$  GPa, and the unit cell volume of the HP phase would correspond to an isotropic pressure of  $P = -0.3$  GPa. However, imposing an isotropic stress on ZIF-8 does not lead to imidazolate reorientation, but on the contrary, the unit cell expands homogeneously, without any “swing” of the linker. The AP-HP transition is thus not due merely to an isotropic stress.

### 2.2. First Principles MD of Guest-free Host

In order to look at the nature of thermal motion of the imidazolate linker, I ran first-principles MD simulations of the empty AP ZIF-8 structure in the (*N*, *V*, *T*) ensemble, at temperatures of 77, 150 and 300 K. The spontaneous “swinging” motion of the imidazolate linkers is observed in all three trajectories. It is then characterized by the dihedral angle  $\varphi$  Zn<sub>3</sub>-Zn<sub>2</sub>-Zn<sub>1</sub>-CH<sub>3</sub> of the imidazolate around the Zn<sub>1</sub>-Zn<sub>2</sub> axis (see Figure S4), where the “reference” of 0° is the 6-ring of Zn (i.e. the window connecting the cages). In the crystallographic AP structure, the window is not perfectly planar ( $\varphi \approx 7^\circ$ ), while in the crystallo-

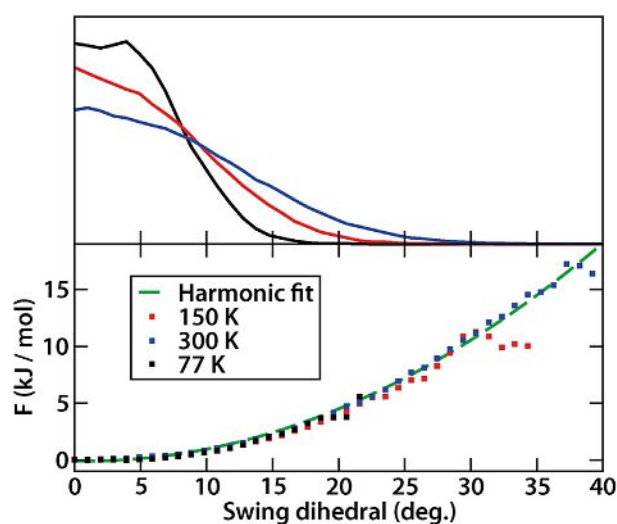


**Figure 2.** Top: histogram of the imidazolate swing angle  $\varphi$  (in degrees), as a function of temperature. Bottom: potential of mean force as a function of the dihedral angle.

graphic HP structure,  $\varphi \approx 35^\circ$ . Figure 2 shows histograms of values taken by  $\varphi$  during our dynamics, where the thermally-activated swinging motions are seen to increase in amplitude with temperature:  $\approx 15^\circ$  at 77 K,  $\approx 20^\circ$  at 150 K and  $\approx 25^\circ$  at 300 K. However, the distribution is in all cases centered around  $\varphi = 0^\circ$ , and never reaches the value of  $35^\circ$  observed in the HP structure.

On the lower panel of Figure 2, we see the potential of mean force (PMF) as a function of dihedral angle,  $F(\varphi) = -kT \log P(\varphi)$ , obtained from the histograms above. The profiles obtained at different temperatures coincide and the free energy is quadratic, which showing that the “thermal swinging motion” seen in the empty host is a soft vibration mode of wide amplitude. The frequency of vibration, as calculated from the MD simulations, is very low at  $\nu_{\text{swing}} = 60(\pm 10) \text{ cm}^{-1}$ . The nature of this motion is in good agreement the experimentally observed peak at 1.95 THz by terahertz time-domain spectroscopy,<sup>[38]</sup> and with the low-frequency terahertz vibrations observed experimentally in guest-free ZIF-8 by inelastic neutron scattering at room temperature, and studied by static DFT calculations in the limit of the harmonic regime.<sup>[39]</sup> The same modes were also shown to be linked to the know shear-instability of ZIF-8, and its pressure-induced amorphization through shear softening.<sup>[40]</sup>

Moreover, the study of the correlations between the motions of the various methylimidazolate linkers shows that they are totally uncorrelated—as is reflection on the matrix of correlation plots at 77 K shown in Figure S2. We also see from Figure 2 that the energy needed to bring one imidazolate linker from  $0^\circ$  to  $35^\circ$  is  $\approx 15 \text{ kJ mol}^{-1}$ . That value is of the same order of magnitude as adsorption enthalpies, explains why guest adsorption can trigger such a large swing motion of the ZIF-8 imidazolate linker, compared to the amplitude of thermal motions.

### 2.3. Grand Canonical Monte Carlo

I then performed grand canonical Monte Carlo simulations of  $N_2$  adsorption in ZIF-8, using the two crystallographic structures AP and HP (Figure S3). These confirmed the findings by Düren et al.<sup>[28]</sup> that while GCMC isotherms in the AP structure describe reasonably the first part of the isotherm, they fail to reproduce the saturation uptake, which is on the other hand reasonably described by GCMC simulations using the HP structure. However, it is clear from the higher-resolutions isotherms published by Calero et al.<sup>[30]</sup> that in the intermediate pressure range, neither the isotherm of the rigid AP or rigid HP structures reproduce the experimental results. In addition, GCMC simulations were also performed at high loading in using two hypothetical structures: one with the AP atomic positions but HP unit cell parameters, and one with HP atomic positions but AP unit cell parameters (red and pink points near  $P = P_0$  on Figure S3). The purpose of these is to check whether the adsorption properties of the two phases are dominated by their linker positions or the total unit cell volume. We can see that the effect of unit cell volume change is marginal, confirming that the main effect is that of the swing of the imidazolate linkers.

### 2.4. First-principles MD with Guest Molecules

The behavior of ZIF-8 at intermediate  $N_2$  loading was then investigated by means of first-principles molecular dynamics. Starting configurations were taken from GCMC simulations, with 11, 27, 41, and 49  $N_2$  molecules adsorbed per unit cell, at a temperature of 77 K. From the analysis of these trajectories, Figure 3 presents the histograms of the imidazolate swing angle  $\varphi$ , for all four loadings and compared to the empty host. We see that at low loading (11  $N_2$ ), the adsorbed molecules have limited effect on the imidazolate linker, increasing slightly the amplitude of swing motions (with a half-width going from  $8^\circ$  to  $12^\circ$ ) but the distribution remains centered near  $0^\circ$ . At higher loading (27, 41, and 49  $N_2$  molecules), we see an impor-

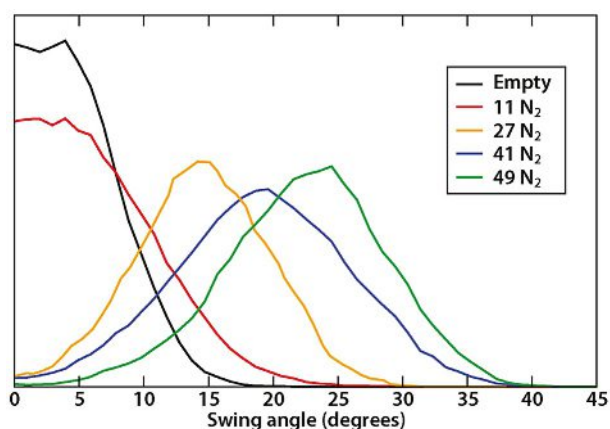


**Figure 3.** Histograms of the swing angle of the imidazolate linkers, for ZIF-8 with various quantities of  $N_2$  adsorbed at 77 K.

tant change in the nature of the distribution of swing angles: its maximum shifts from  $\approx 0^\circ$  to  $14^\circ$ ,  $20^\circ$ , and  $25^\circ$  (for 27, 41, and 49 guest molecules, respectively). This is the manifestation of the opening of the windows, which occurs as a gradual transformation of the ZIF-8 structure upon adsorption, from the guest-free metastable AP structure to a guest-loaded HP structure with open windows. It contrasts with the previous picture of an abrupt, first-order adsorption-induced transition<sup>[28,41]</sup> between preexisting phases of the bare ZIF-8 framework. This is consistent with our quantum chemical calculations, which show that the HP structure is not metastable in the absence of guest molecules. It is also in good agreement with recent indirect experimental evidence obtained by  $^2H$  NMR<sup>[42]</sup> and later by in situ inelastic neutron scattering,<sup>[43]</sup> showing that the linker swing motion is retained at full loading—although the exact nature of the transition and behaviour at intermediate loading was not detailed.

It should be noted that at all loadings simulated, a few events of diffusion of  $N_2$  through the six-ring windows of ZIF-8 are observed. From the “rigid” AP structure,  $N_2$  diffusion is not expected from geometric considerations, as the window diameter of 3.4 Å is smaller than the  $N_2$  kinetic diameter of 3.6 Å. Thus, this shows that even a “small” swing amplitude (of the order of  $15^\circ$ ) is enough to allow rather “fast” diffusion of  $N_2$  in the pores of ZIF-8, which is observed twice in a 18 ps dynamics at 77 K. Furthermore, I analyzed the spatial distribution of  $N_2$  molecules adsorbed at loadings of  $N=41$  and  $N=49$  molecules per unit cell. In order to get the necessary statistics, GCMC results were used for that analysis. They confirm that the opening of the ZIF-8 window allows for a denser packing of  $N_2$ , with the possibility of having 2 molecules per window (at  $N \approx 49$  in the HP structure) against only 1 molecule per window (at  $N \approx 41$  in the AP structure). This packing effect can explain the observed steps on the experimental adsorption-desorption isotherms,<sup>[27–30]</sup> similarly to what has been demonstrated for other flexible porous materials in both theoretical<sup>[44,45]</sup> and experimental<sup>[46]</sup> works.

### 2.5. Linker Functionalization

Finally, I studied the influence of the nature of the ZIF-8 linker by comparing the swing motions of ZIF-8 (whose linker is 2-methylimidazole) with a ZIF with the same sodalite (sod) topology but built on an unsubstituted imidazolate linker—a structure similar to that of material SALEM-2, obtained from ZIF-8 by post-synthetic exchange of the linkers.<sup>[35]</sup> Quantum chemical calculations show that in SALEM-2 the most stable structure still resembles the AP structure, with a swing angle close to zero. However, molecular dynamics at 77 K reveals (Figure 4) that the swing motions are of a much larger amplitude for SALEM-2 than for ZIF-8. In fact, at 77 K, the “thermal” swing motion goes all the way up to  $35^\circ$  (instead of  $15^\circ$  for ZIF-8). The free energy required for a rotation of the linker from  $0^\circ$  to  $35^\circ$  is a mere  $3.5 \text{ kJ mol}^{-1}$  for SALEM-2, compared to  $15 \text{ kJ mol}^{-1}$  for ZIF-8. This “extra” stabilization of the “AP” structure of ZIF-8 (compared to its unsubstituted variant) can be ascribed to the dispersive interactions between the methyl

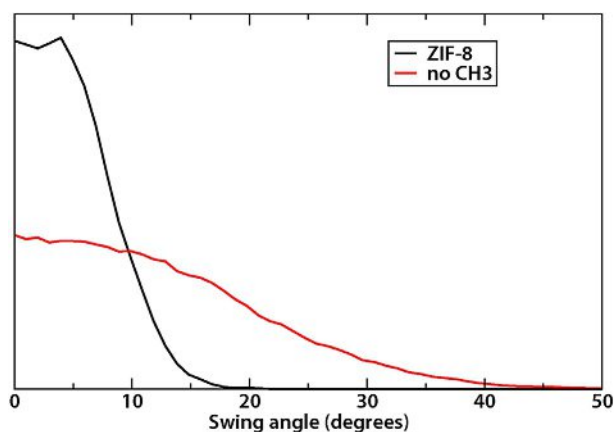


Figure 4. Histograms of the swing angle of the imidazolate linkers, for ZIF-8 (black) and SALEM-2 (red) at 77 K.

groups and the neighboring windows, which favor the in-plane configuration. As a consequence, I predict that the “swing effects” in SALEM-2 are much less severe, if they are visible at all, than in ZIF-8. This also shows that the “swing effect” of ZIF-8, which were studied here, is not a universal phenomenon for ZIF structures, but linked to the specific nature of the ZIF-8 framework.

### 3. Conclusions

In conclusion, combined quantum chemistry calculations and first-principles molecular dynamics simulations demonstrate that the “swing effect” or “window opening” in ZIF-8 is in fact a gradual adsorption-induced deformation of the ZIF-8 framework. The “open window” (or “high pressure”) structure is not metastable in the absence of adsorbate, and the opening transition is continuous and not of the first order (as was suggested in prior literature). This gradual deformation leads to stepped isotherms in some cases because of packing effects of the adsorbed phase. Experimentally, stepped isotherms have been observed for small molecules at low temperature, which is exactly when such packing effects can be expected to dominate (dense and well-organized adsorbed phases). Thus, GCMC simulations at fixed volumes, even when considering two (AP and HP) or more phases, are not well-suited to study guest adsorption in ZIF-8. Studies in the osmotic ensemble are required for a complete thermodynamic description of adsorption. Furthermore, it is shown that extent of the swinging motions of the imidazolate linker depend largely on the microscopic nature of the linker, and predict that the “swing effect” would be much less important on a ZIF-8 with unsubstituted imidazole linker. This opens the way to fine-tuning of the ZIFs’ adsorption and permeation properties by chemical tuning, pre- or post-synthesis, of their linkers. First-principles molecular dynamics is a useful tool to investigate the microscopic behavior of these soft porous materials and predict the impact of adsorbates on their structure.

## Computational Methods

### Quantum Chemistry Calculations

The structures of all MOF materials considered were fully relaxed by optimizing both atomic positions and unit cell parameters simultaneously, starting from the experimental crystallographic structure. First-principles calculations were performed in the density functional theory approach with periodic unit cell, full use of the crystal’s symmetry elements and localized basis sets as implemented in the CRYSTAL14 code.<sup>[47]</sup> The B3LYP hybrid exchange-correlation functional<sup>[48]</sup> was used, with empirical correction for the dispersive interactions following the Scheme of Grimme.<sup>[49]</sup> All electron basis sets were used for all atoms: H (3-1p1G), C (6-31d1G), N (6-31d1G)<sup>[50]</sup> and Zn (86-411d31G).<sup>[51]</sup> The accuracy of this methodology is now well established for the calculation of MOF and ZIF structures, their relative energies,<sup>[52]</sup> and elastic constants.<sup>[53,54]</sup> Unit cell parameters obtained for ZIF-8 was 16.86 Å (vs. 16.99 Å experimentally),<sup>[5]</sup> while for SALEM-2 it is 17.01 Å (experimentally 16.83 Å)<sup>[35]</sup>—although that latter experimental value was determined not for a pure imidazolate-based SALEM-2 but for a mixed-ligand ZIF of composition Zn(im)<sub>1.3</sub>(mim)<sub>0.3</sub>. Calculations were repeated with the PBESOL0 exchange-correlation functional, and the conclusions were identical. After full optimization in the crystal’s symmetry group, negative frequencies remained corresponding to the free rotation of the ZIF-8 methyl top.

### First-principles Molecular Dynamics

First-principles molecular dynamic (FPMD) simulations of the ZIF-8 and SALEM-2 empty frameworks, as well as the ZIF-8 framework with various quantities of adsorbed N<sub>2</sub>, were performed with Born–Oppenheimer dynamics based on density functional theory for the calculation of atomic forces. They were carried out using the QUICKSTEP/CP2K package,<sup>[55]</sup> which is based on a hybrid Gaussian plane-wave approach combining a Gaussian basis for the wave functions with an auxiliary plane wave basis set for the representation of the density.<sup>[56]</sup> The gradient-corrected BLYP functional<sup>[57,58]</sup> was employed with empirical correction for the dispersive interactions using the Grimme “D3” method.<sup>[59]</sup> The cutoff for the density plane-wave basis set was set to 400 Ry at the finest level, and double- $\zeta$  valence polarized (DZVP) basis sets were used for all atoms.

All molecular simulations were performed using periodic boundary conditions on a single unit cell of the material (ZIF-8 or SALEM-2). Hydrogen atoms were deuterated to allow for a larger time step (0.5 fs) in the integration of the equations of motion. Simulations were run in the canonical ensemble ( $N, V, T$ ), and the temperature was controlled by a Nosé–Hoover thermostat chain.<sup>[60]</sup> For each simulation, an initial equilibration period of 5 ps was used, with a thermostat time constant of 400 fs, before a production run lasting 15 to 25 ps, during which the thermostat time constant is set to 1000 fs. Results were then checked against shorter ( $N, P, T$ ) runs (10 ps, with 250 fs thermostat time constant and 1 ps barostat time constant) to validate the little influence of the unit cell volume change on the results obtained. For example, for the empty ZIF-8 framework at 77 K, constant-pressure simulations found an average unit cell parameter of 16.94 Å (vs. 16.86 Å for the energy-minimized structure).

From the molecular simulations, the dihedral angle  $\varphi$  was used to characterize the swing of each imidazolate linker (Zn3–Zn2–Zn1–CH<sub>3</sub>; see Figure S4). The frequency of the swinging motion  $\nu_{\text{swing}}$  was then calculated from the trajectories, by Fourier transform of

the  $\varphi(t)$  autocorrelation function, and the width of the FT peak gives the uncertainty of  $\pm 10 \text{ cm}^{-1}$ .

### Grand Canonical Monte Carlo

To characterize the thermodynamics of adsorption of  $\text{N}_2$  in the rigid ZIF-8 AP and HP structures, force field-based Monte Carlo simulations were performed in the grand canonical ensemble. The  $\text{N}_2$  molecules were described by a rigid two points and three charges TraPPE model.<sup>[61]</sup> The ZIF-8 structure was described as in Ref. [62]. These force field parameters are presented in the Supporting Information. Lorentz-Berthelot rules were used to calculate ZIF- $\text{N}_2$  Lennard-Jones parameters. Series of GCMC simulations were performed at various values of  $\text{N}_2$  fugacity, which was then related to gas pressure by the ideal gas law. Long-range electrostatic interactions were taken into account using the Ewald summation technique. In order to improve the efficiency of the calculations, electrostatic and repulsion-dispersion interaction energies between the rigid ZIF-8 framework and adsorbed  $\text{N}_2$  molecules were precomputed on a grid (with a grid mesh of 0.1 Å) and stored for use during the simulation.

### Acknowledgements

Funding from the Agence Nationale de la Recherche under project "SOFT-CRYSTAB" (ANR-2010-BLAN-0822) is acknowledged. This work was performed using HPC resources from GENCI (project A0010807069). I thank Aurélie Ortiz, Anne Boutin, Alain Fuchs, Alex Neimark, and Peter Ravikovitch for fruitful discussions.

**Keywords:** adsorption · first-principles simulations · flexibility · metal–organic frameworks · molecular dynamics

- [1] S. Horike, S. Shimomura, S. Kitagawa, *Nat. Chem.* **2009**, *1*, 695–704.
- [2] O. K. Farha, J. T. Hupp, *Acc. Chem. Res.* **2010**, *43*, 1166–1175.
- [3] G. Férey, *Chem. Soc. Rev.* **2008**, *37*, 191–214.
- [4] D. J. Tranchemontagne, J. L. Mendoza-Cortes, M. O’Keeffe, O. M. Yaghi, *Chem. Soc. Rev.* **2009**, *38*, 1257–1283.
- [5] K. S. Park, Z. Ni, A. P. Côté, J. Y. Choi, R. Huang, F. J. Uribe-Romo, H. K. Chae, M. O’Keeffe, O. M. Yaghi, *Proc. Natl. Acad. Sci. USA* **2006**, *103*, 10186.
- [6] J.-P. Zhang, A.-X. Zhu, R.-B. Lin, X.-L. Qi, X.-M. Chen, *Adv. Mater.* **2011**, *23*, 1268–1271.
- [7] A. Phan, C. J. Doonan, F. J. Uribe-Romo, C. B. Knobler, M. O’Keeffe, O. M. Yaghi, *Acc. Chem. Res.* **2010**, *43*, 58–67.
- [8] J.-P. Zhang, Y.-B. Zhang, J.-B. Lin, X.-M. Chen, *Chem. Rev.* **2012**, *112*, 1001–1033.
- [9] I. A. Baburin, S. Leoni, G. Seifert, *J. Phys. Chem. B* **2008**, *112*, 9437–9443.
- [10] L. B. du Bourg, A. U. Ortiz, A. Boutin, F.-X. Coudert, *APL Mater.* **2014**, *2*, 124110.
- [11] J. T. Hughes, T. D. Bennett, A. K. Cheetham, A. Navrotsky, *J. Am. Chem. Soc.* **2013**, *135*, 598–601.
- [12] R. Banerjee, A. Phan, B. Wang, C. Knobler, H. Furukawa, M. O’Keeffe, O. M. Yaghi, *Science* **2008**, *319*, 939–943.
- [13] G. Lu, J. T. Hupp, *J. Am. Chem. Soc.* **2010**, *132*, 7832–7833.
- [14] N. Liédana, A. Galve, C. Rubio, C. Téllez, J. Coronas, *ACS Appl. Mater. Interfaces* **2012**, *4*, 5016–5021.
- [15] K. Li, D. H. Olson, J. Seidel, T. J. Emge, H. Gong, H. Zeng, J. Li, *J. Am. Chem. Soc.* **2009**, *131*, 10368–10369.
- [16] C. Gücüyener, J. van den Bergh, J. Gascon, F. Kapteijn, *J. Am. Chem. Soc.* **2010**, *132*, 17704–17706.
- [17] H. Bux, A. Feldhoff, J. Cravillon, M. Wiebcke, Y.-S. Li, J. Caro, *Chem. Mater.* **2011**, *23*, 2262–2269.
- [18] T.-H. Bae, J. S. Lee, W. Qiu, W. J. Koros, C. W. Jones, S. Nair, *Angew. Chem. Int. Ed.* **2010**, *49*, 9863–9866; *Angew. Chem.* **2010**, *122*, 10059–10062.
- [19] Y. Pan, Y. Liu, G. Zeng, L. Zhao, Z. Lai, *Chem. Commun.* **2011**, *47*, 2071.
- [20] M. J. C. Ordoñez, K. J. Balkus, J. P. Ferraris, I. H. Musselman, *J. Membr. Sci.* **2010**, *361*, 28–37.
- [21] G. Lu, O. K. Farha, W. Zhang, F. Huo, J. T. Hupp, *Adv. Mater.* **2012**, *24*, 3970–3974.
- [22] K. W. Chapman, G. J. Halder, P. J. Chupas, *J. Am. Chem. Soc.* **2009**, *131*, 17546–17547.
- [23] S. Cao, T. D. Bennett, D. A. Keen, A. L. Goodwin, A. K. Cheetham, *Chem. Commun.* **2012**, *48*, 7805.
- [24] X. Wu, J. Huang, W. Cai, M. Jaroniec, *RSC Adv.* **2014**, *4*, 16503–16511.
- [25] K. Zhang, R. P. Lively, C. Zhang, R. R. Chance, W. J. Koros, D. S. Sholl, S. Nair, *J. Phys. Chem. Lett.* **2013**, *4*, 3618–3622.
- [26] R. J. Verploegh, S. Nair, D. Sholl, *J. Am. Chem. Soc.* **2015**, *137*, 15760–15771.
- [27] S. A. Moggach, T. Bennett, A. Cheetham, *Angew. Chem. Int. Ed.* **2009**, *48*, 7087–7089; *Angew. Chem.* **2009**, *121*, 7221–7223.
- [28] D. Fairen-Jimenez, S. A. Moggach, M. T. Wharmby, P. A. Wright, S. Parsons, T. Düren, *J. Am. Chem. Soc.* **2011**, *133*, 8900–8902.
- [29] D. Fairen-Jimenez, R. Galvelis, A. Torrisi, A. D. Gellan, M. T. Wharmby, P. A. Wright, C. Mellot-Draznieks, T. Düren, *Dalton Trans.* **2012**, *41*, 10752–10762.
- [30] C. O. Ania, E. García-Pérez, M. Haro, J. J. Gutiérrez-Sevillano, T. Valdés-Solís, J. B. Parra, S. Calero, *J. Phys. Chem. Lett.* **2012**, *3*, 1159–1164.
- [31] S. Aguado, G. Bergeret, M. P. Titus, V. Moizan, C. Nieto-Draghi, N. Bats, D. Farrusseng, *New J. Chem.* **2011**, *35*, 546–550.
- [32] J. van den Bergh, C. Gücüyener, E. A. Pidko, E. J. M. Hensen, J. Kapteijn, F. Gascon, *Chem. Eur. J.* **2011**, *17*, 8832–8840.
- [33] P. Zhao, G. I. Lampronti, G. O. Lloyd, M. T. Wharmby, S. Facc, A. K. Cheetham, S. A. T. Redfern, *Chem. Mater.* **2014**, *26*, 1767–1769.
- [34] Y. Du, B. Wooler, M. Nines, P. Kortunov, C. S. Paur, J. Zengel, S. C. Weston, P. I. Ravikovitch, *J. Am. Chem. Soc.* **2015**, *137*, 13603–13611.
- [35] O. Karagiari, M. B. Lalonde, W. Bury, A. A. Sarjeant, O. K. Farha, J. T. Hupp, *J. Am. Chem. Soc.* **2012**, *134*, 18790–18796.
- [36] A. Schneemann, V. Bon, I. Schwedler, I. Senkovska, S. Fischer, R. A. Kaskel, *Chem. Soc. Rev.* **2014**, *43*, 6062–6096.
- [37] T. Loiseau, C. Serre, C. Huguenard, G. Fink, F. Taulelle, M. Henry, T. Baille, G. Férey, *Chem. Eur. J.* **2004**, *10*, 1373–1382.
- [38] N. Y. Tan, M. T. Ruggiero, C. Orellana-Tavra, T. Tian, A. D. Bond, T. M. Korter, D. Fairen-Jimenez, J. A. Zeitler, *Chem. Commun.* **2015**, *51*, 16037–16040.
- [39] M. R. Ryder, B. Civalieri, T. D. Bennet, S. Henke, S. Rudić, G. Cinque, F. Fernandez-Alonso, J.-C. Tan, *Phys. Rev. Lett.* **2014**, *113*, 215502.
- [40] A. U. Ortiz, A. Boutin, A. H. Fuchs, F.-X. Coudert, *J. Phys. Chem. Lett.* **2013**, *4*, 1861–1865.
- [41] L. Zhang, Z. Hu, J. Jiang, *J. Am. Chem. Soc.* **2013**, *135*, 3722–3728.
- [42] D. I. Kolokolov, A. G. Stepanov, H. Jobic, *J. Phys. Chem. C* **2015**, *119*, 27512–27520.
- [43] M. E. Casco, Y. Q. Cheng, L. L. Daemen, D. Fairen-Jimenez, E. V. Ramos-Fernández, A. J. Ramirez-Cuesta, J. Silvestre-Albero, *Chem. Commun.* **2016**, *52*, 3639–3642.
- [44] D. Bousquet, F.-X. Coudert, A. G. J. Fossati, A. V. Neimark, A. H. Fuchs, A. Boutin, *J. Chem. Phys.* **2013**, *138*, 174706.
- [45] D. Bousquet, F.-X. Coudert, A. Boutin, *J. Chem. Phys.* **2012**, *137*, 044118.
- [46] F. Salles, G. Maurin, C. Serre, P. L. Llewellyn, C. Knöfel, H. J. Choi, Y. Filinchuk, L. Oliviero, A. Vimont, J. R. Long, G. Férey, *J. Am. Chem. Soc.* **2010**, *132*, 13782–13788.
- [47] R. Dovesi, R. Orlando, B. Civalieri, C. Roetti, V. R. Saunders, C. M. Zicovich-Wilson, *Z. Kristallogr.* **2005**, *220*, 571.
- [48] A. D. Becke, *J. Chem. Phys.* **1993**, *98*, 5648.
- [49] S. Grimme, *J. Comput. Chem.* **2006**, *27*, 1787.
- [50] C. Gatti, V. R. Saunders, C. Roetti, *J. Chem. Phys.* **1994**, *101*, 10686–10696.
- [51] J. E. Jaffe, A. C. Hess, *Phys. Rev. B* **1993**, *48*, 7903.
- [52] A. M. Walker, B. Civalieri, B. Slater, C. Mellot-Draznieks, F. Corà, C. M. Zicovich-Wilson, G. Román-Pérez, J. M. Soler, J. D. Gale, *Angew. Chem. Int. Ed.* **2010**, *49*, 7501; *Angew. Chem.* **2010**, *122*, 7663.
- [53] J.-C. Tan, B. Civalieri, C.-C. Lin, L. Valenzano, R. Galvelis, P.-F. Chen, T. D. Bennett, C. Mellot-Draznieks, C. M. Zicovich-Wilson, A. K. Cheetham, *Phys. Rev. Lett.* **2012**, *108*, 095502.

- [54] A. U. Ortiz, A. Boutin, A. H. Fuchs, F.-X. Coudert, *Phys. Rev. Lett.* **2012**, *109*, 195502.
- [55] J. VandeVondele, M. Krack, F. Mohamed, M. Parrinello, T. Chassaing, J. Hutter, *Comput. Phys. Commun.* **2005**, *167*, 103.
- [56] G. Lippert, J. Hutter, M. Parrinello, *Mol. Phys.* **1997**, *92*, 477.
- [57] A. D. Becke, *Phys. Rev. A* **1988**, *38*, 3098.
- [58] C. Lee, W. Yang, R. G. Parr, *Phys. Rev. B* **1988**, *37*, 785.
- [59] S. Grimme, J. Antony, S. Ehrlich, H. Krieg, *J. Chem. Phys.* **2010**, *132*, 154104.
- [60] S. Nosé, *J. Chem. Phys.* **1984**, *81*, 511.
- [61] J. J. Potoff, J. I. Siepmann, *AIChE J.* **2001**, *47*, 1676–1682.
- [62] A. U. Ortiz, A. P. Freitas, A. Boutin, A. H. Fuchs, F.-X. Coudert, *Phys. Chem. Chem. Phys.* **2014**, *16*, 9940–9949.

---

Manuscript received: April 29, 2017  
Revised manuscript received: June 21, 2017  
Accepted manuscript online: July 3, 2017  
Version of record online: August 4, 2017